Virology 535 (2019) 241–254

Contents lists available at ScienceDirect

Virology

journal homepage: www.elsevier.com/locate/virology

Magnaporthe oryzae chrysovirus 1 strain D confers growth inhibition to the host fungus and exhibits multiform viral structural proteins

Tomoya Higashiura[a], Yu Katoh[a], Syun-ichi Urayama[a], Osamu Hayashi[e], Mitsuhiro Aihara[a], Toshiyuki Fukuhara[a], Shin-ichi Fuji[c], Takashi Kobayashi[d], Shu Hase[d], Tsutomu Arie[b], Tohru Teraoka[b], Ken Komatsu[b], Hiromitsu Moriyama[a,*]

[a] Laboratory of Molecular and Cellular Biology, Department of Applied Biological Sciences, Tokyo University of Agriculture and Technology, 3-5-8, Saiwaicho, Fuchu, Tokyo, Japan
[b] Laboratory of Plant Pathology, Department of Applied Biological Sciences, Tokyo University of Agriculture and Technology, 3-5-8, Saiwaicho, Fuchu, Tokyo, Japan
[c] Faculty of Bioresource Science, Akita Prefectural University, 241-438, Kaidobata Nishi Shinjo Nakano, Akita, Japan
[d] Laboratory of Plant Pathology, Faculty of Agriculture, Yamagata University, 1-23, Wakabatyo, Tsuruoka, Yamagata, Japan
[e] The Institute of Environmental Toxicology, 4321, Uchimoriya-machi, Joso, Ibaraki, Japan

ARTICLE INFO

Keywords:
Mycovirus
DsRNA virus
Chrysovirus cluster II
Attenuation
Magnapothe oryzae
Magnaporthe oryzae chrysovirus 1
Magnaporthe oryzae virus 2
Multi-segmented mycovirus
Yeast heterologous expression assay
Melanin

ABSTRACT

A Japanese isolate of *Magnaporthe oryzae* is infected by Magnaporthe oryzae chrysovirus 1-D (MoCV1-D), which is classified in cluster II of the family *Chrysoviridae*. The genome of MoCV1-D consists of five dsRNAs. dsRNAs 1–4 show high identity with those of related MoCV1 viruses, whereas dsRNA5 shows relatively low identity and is sometimes deleted during virus propagation. MoCV1-D causes growth inhibition of its host fungus, and the protein encoded by its dsRNA4 impairs cell growth when expressed in yeast cells. It also causes abnormal pigmentation and colony albinization, and we showed that these phenotypes are associated with reduced accumulation of the melanin biosynthesis intermediate scytalone. MoCV1-D exhibits multiform viral structural proteins during prolonged culture. The original host isolate is co-infected with MoCV1-D, a victorivirus, and a partitivirus, and these mycoviruses are detected in cell-free supernatant fractions after prolonged liquid culturing. Hyphal fusion experiments demonstrated that MoCV1-D is transmissible via anastomosis.

1. Introduction

Viruses that infect fungi, called mycoviruses, have been found in numerous fungal species (Bao and Roossinck, 2013; Dawe and Nuss, 2013; Ghabrial et al., 2013; Hillman and Cai, 2013). Mycoviruses are primarily classified into three groups based on their genomic structure: single-stranded DNA (ssDNA), single-stranded RNA (ssRNA), and double-stranded RNA (dsRNA). Mycoviruses with dsRNA genomes are currently classified into six families based on the amino acid sequence of the RNA-dependent RNA polymerase (RdRp), the genomic structure, the virion structure, and the presence or absence of coat protein. These families are: the *Totiviridae* (nonsegmented genome), the *Partitiviridae* (2 segments), the *Megabirnaviridae* (2 segments), the *Chrysoviridae* (3–5 segments), the *Quadriviridae* (4 segments) and the *Reoviridae* (10–12 segments) (Ghabrial and Suzuki, 2009; Nibert et al., 2013; Ghabrial et al., 2015).

Since some mycoviruses can reduce the virulence of plant pathogenic fungi, they have potential as biological control agents (Huang and Ghabrial, 1996; Yu et al., 2013). The best example is the attenuation of the chestnut blight fungus, *Cryphonectria parasitica*, by the ssRNA mycovirus Cryphonectria hypovirus 1 (CHV1-EP713) (Nuss, 2005). CHV1-EP713-infected strains of *C. parasitica* were used as donors to transmit CHV1-EP713 to virulent strains of *C. parasitica* in Europe and the United States (Heiniger and Rigling, 1994; Milgroom and Cortesi, 2004). Another example is the attenuation of *Helminthosporium victoriae*, which causes Victoria blight disease in oats, by Helminthosporium victoriae virus 190S (HvV190S) and Helminthosporium victoriae chrysovirus HvV145S (Sanderlin and Ghabrial, 1978; Litzenberger, 1949). HvV190S is a type species of the genus *Victorivirus* in the family *Totiviridae*, and has a nonsegmented dsRNA genome (5.2 kbp) with two large overlapping open reading frames (ORFs) (Huang and Ghabrial, 1996). HvV145S is in the genus *Chrysovirus*, family *Chrysoviridae*, and has four dsRNA segments (2.7, 2.9, 3.1 and 3.6 kbp), each with a unique, monocistronic sequence (Ghabrial et al., 2002, 2018; Jiang and Ghabrial, 2004). HvV190S is the primary cause of attenuation of *H. victoriae*, while HvV145S does not appear to affect colony morphology

* Corresponding author.
E-mail address: hmori714@cc.tuat.ac.jp (H. Moriyama).

https://doi.org/10.1016/j.virol.2019.07.014
Received 22 January 2019; Received in revised form 11 July 2019; Accepted 14 July 2019
Available online 15 July 2019

of the infected fungal isolates (Ghabrial, 2008).

Magnaporthe oryzae, the causal agent of rice blast disease, is the most destructive pathogen of rice worldwide. A number of mycoviruses have been reported to infect *M. oryzae*, including Magnaporthe oryzae viruses 1, 2, and 3 (MoV1, 2, and 3) in the genus *Victorivirus* (Yokoi et al., 2007; Maejima et al., 2008; Tang et al., 2015), Magnaporthe oryzae partitivirus 1 in the family *Partitiviridae* (Du et al., 2016), and Magnaporthe oryzae chrysovirus 1 (MoCV1) in cluster II of the family *Chrysoviridae* (Urayama et al., 2010, 2012, 2014a). Two other kinds of *M. oryzae* viruses have been reported: a mycovirus related to plant viruses of the family *Tombusviridae* (Magnaporthe oryzae virus A) (Ai et al., 2016) and a (+)ssRNA mycovirus closely related to the ourmia-like viruses (Magnaporthe oryzae ourmia-like virus 1) (Illana et al., 2017). Among these, MoCV1 strains A and B (MoCV1-A, MoCV1-B) were the first reported to cause hypovirulence associated traits in *M. oryzae*, such as impaired growth of host cells, altered colony morphology, and reduced pigmentation. The strain MoCV1-C was found in a rice blast fungus that was co-infected with a victorivirus (MoV3) in China (Tang et al., 2015). Very recently, we reported that MoCV1-A infection generally confers hypovirulence to the fungus, but could also be a driving force in generating physiological diversity, leading to the development of new pathogenic races of the fungus (Aihara et al., 2018). In another example of a mycovirus altering the pathogenicity of its host, we reported that *Alternaria alternata* chrysovirus 1 (AaCV1), which is also in cluster II of the *Chrysoviridae*, exhibits two contrasting effects: it impairs the growth of the host fungus while rendering the fungus hypervirulent to the plant, with increased production of a host-specific toxin (Okada et al., 2018).

Many new members have been added to cluster II of the family *Chrysoviridae* in recent years. Among these, four mycoviruses are reported to alter the pathogenicity of their host fungi against plants: MoCV1-A (Aihara et al., 2018), AaCV1 (Okada et al., 2018), Fusarium graminearum mycovirus-China 9 (FgV-Ch-9; Darissa et al., 2011; Bormann et al., 2018), and Aspergillus thermomutatus Chrysovirus 1 (AthCV1; Ejmal et al., 2018). Our experiments using a yeast heterologous expression system revealed that the ORF4 protein of MoCV1-A and the ORF2 protein of AaCV1 were responsible for growth inhibition of the yeasts *Saccharomyces cerevisiae* (Urayama et al., 2012, 2016a, Okada et al., 2018) and *Cryptococcus neoformance* (Urayama et al., 2014b). Nine other mycoviruses in cluster II of the *Chrysoviridae* encode a viral proteins with significant similarity to the MoCV1-A ORF4 protein, suggesting that these viruses may preserve proteins related to hypovirulence.

Recently, we used RT-PCR to detect MoCV1-related viruses in Japanese isolates of *M. oryzae* (Komatsu et al., 2016). Here we report on the molecular characteristics of a new strain, referred to as Magnaporthe oryzae chrysovirus 1 strain D (MoCV1-D), found in the Japanese *M. oryzae* isolate APU10-199A.

2. Materials and methods

2.1. Fungal strains and culture conditions

The *Magnaporthe oryzae* isolate APU10-199A was obtained from symptomatic leaves of the *japonica* rice cultivar Akitakomachi in Odate, Akita Prefecture, Japan. The virus-free *M. oryzae* isolate P2 (MAFF235001) (Kamakura et al., 2002) was used as a recipient for virus infection, after introduction of a hygromycin-resistance (*hph*) gene. *M. oryzae* Japanese field isolate Ina168 was used for transformation of ORF4 of MoCV1-D. The *M. oryzae* isolates were grown on potato dextrose agar (PDA) or oatmeal agar (OMA) media (Yang et al., 2009) at 26 °C for 10 days. For liquid cultures, mycelia were incubated in flasks containing 0.5% yeast extract and 2% glucose liquid broth (YG broth), with reciprocal shaking (60 strokes per min) at 26 °C for 10 days. Fermentation reactors (2.5 liters; Able Biott, Japan) were also used for fungal cultivation in YG broth (1.5 liters) at 26 °C, with agitation at 100 rpm and air introduced at 1.5 liters/min.

The *S. cerevisiae* strain W303-1A (*MAT*a, *ura*3 *his*3 *leu*2 *trp*1 *ade*2 *can*1 [L-A-o]) was produced previously (Urayama et al., 2012) and is based on strain W303-1A [L-A], a gift from emeritus Prof. A. Toh-e. W303-1A was cultured in standard yeast media (Sherman, 2002).

2.2. Extraction and purification of viral dsRNA from host fungi and from culture supernatants

Viral dsRNA was isolated from the host fungi using a micro-spin column-based method (Okada et al., 2015). In brief, 0.1 g (fresh weight) of mycelia cultured in YG broth was pulverized in liquid nitrogen then mixed with 0.5 ml of 2 × STE buffer (200 mM NaCl, 20 mM Tris-HCl pH 8.0, 2 mM EDTA pH 8.0) containing 1% SDS and 0.5 ml 1:1 phenol/chloroform. The mixture was vortexed then centrifuged at 15,000 g for 5 min. The supernatant was transferred to a spin-column packed with cellulose D (Advantec, Japan) and washed with 1 × STE containing 16.6% ethanol. The purified dsRNA was eluted in 0.4 ml of 1 × STE and checked by electrophoresis in 1% (w/v) agarose gels or 5% (w/v) polyacrylamide gels stained with ethidium bromide (0.5 μg/ml). For extraction of nucleic acids from culture supernatants, the harvested liquid culture was mixed with SDS (1% final concentration) and an equal volume of 1:1 phenol:chloroform. The mixture was vortexed, centrifuged at 15,000 g for 5 min, and the supernatant was electrophoresed as described above, without spin-column purification.

2.3. Isolation of single conidia

After incubation of the APU10-199A isolate on OMA, conidium formation was induced by placing the OMA plate under UV-A light for 3 days. The conidia were suspended in sterilized distilled water and single conidia were isolated using a joystick-micromanipulation system (MN-151, NARISHIGE GROUP, JAPAN).

2.4. cDNA cloning, genome sequencing, and phylogenetic analysis

Double-stranded RNAs extracted from the original isolate APU10-199A were used as templates for cDNA synthesis, and a series of overlapping cDNA clones were obtained as described by Aoki et al. (2009). The 5′- and 3′-terminal sequences of each dsRNA segment were determined using the SMARTer® RACE cDNA Amplification Kit according to the manufacturer's protocol (Clontech Laboratories, Inc., Mountain View, CA, US) (Frohman et al., 1988). The estimation of ORFs in the MoCV1-D genome and the similarity search with other mycoviruses were conducted using the GENETYX Ver. 9 software (Genetyx, Tokyo, Japan).

For the phylogenetic analysis, the deduced amino acid sequences of the viral RdRp regions were aligned using Clustal X ver. 2.0 (Thompson et al., 1997). The resultant multiple alignments were trimmed to a core region with 8 conserved motifs using GeneDoc ver. 2.7 (Nicholas et al., 1997). Phylogenetic analyses were conducted with MEGA 7 (Kumar et al., 2016). The LG + G + I amino acid substitution model was assessed by the best-fit method, and the evolutionary history was inferred using the Maximum Likelihood method (Le and Gascuel, 2008).

For MoV2, a sequencing library was generated and analyzed using IonPGM (Life Technologies), then the sequence reads were assembled using a CLC Genomics Workbench (CLC Bio, Aarhus, Denmark). To obtain the full-length dsRNA sequence, the dsRNAs isolated from APU199-10A were subjected to the fragmented and loop-primer ligated dsRNA sequencing (FLDS) method (Urayama et al., 2016b).

2.5. Purification of viruses from mycelia

Mycelia of isolate APU10-199A were cultured in fermenters for 3 or 10 days. Fresh mycelia (10 g) were homogenized in buffer A (0.1 M sodium phosphate, 0.2 M KCl, pH7.4) with a mixer and a French press

(5501-M, Ohtake Works, Tokyo, Japan) set at 120 MPa. After centrifugation (31,200 g, 20 min, 4 °C), the supernatant was ultracentrifuged at 104,000 g for 1 h in a Hitachi CP80WX P80AT rotor to precipitate the viral particles. The particles were resuspended in buffer A, then the two centrifugation steps were repeated to remove unwanted components. The precipitate was suspended in 0.1 M sodium phosphate buffer (pH 7.4), and applied to a sucrose density gradient (100–400 mg/ml) in buffer A, with ultracentrifugation (112,700 g, 2.5 h, 4 °C) using a Hitachi CP80WX P28S swing rotor. The density gradient was fractionated with a Hitachi DGF-U fractionator, and virus-rich fractions (21–24% sucrose) were recovered and ultracentrifuged (104,000 g, 1 h) to precipitate the viral particles. The precipitate was dissolved in buffer A then subjected to CsCl density centrifugation (133,800 g, 24 h, 20 °C). Fractions that contained MoCV1-D or MoV2 were collected and ultracentrifuged (104,000 g, 1 h) to recover the virus particles. The resuspended solutions were stained with 2% uranyl acetate, and the MoCV1-D viral particles were visualized using a transmission electron microscope (JEM1400 Plus, JEOL, Japan).

2.6. Viral protein analysis

Structural proteins in the purified viral preparations were resolved by 8% SDS-PAGE with 25 mM Tris/glycine and 0.1% SDS at 15 mA for 2 h. After electrophoresis, the gels were stained with Bio-Safe Coomassie Brilliant Blue (CBB) (Bio-Rad). Western blotting analysis was performed using rabbit antiserum against the MoCV1-A viral particle, as described previously (Urayama et al., 2010, 2014a). Rabbit antisera against the recombinant MoCV1-D-ORF3 or MoCV1-D-ORF4 proteins (see below) were also used to detect the MoCV1-D viral proteins.

2.7. Production of polyclonal antisera against the recombinant MoCV1-D ORF3 and ORF4 proteins

The recombinant MoCV1-D ORF3 and ORF4 proteins (rORF3p and rORF4p, respectively) were expressed in *Escherichia coli* using a pCold expression system (Takara Bio, Otsu, Japan). Primers used in these experiments are listed in Table S2. The cloning procedures were as described by Urayama et al. (2016a) and the proteins were produced and purified as described by Okada et al. (2018). A rabbit anti-6 His antibody (Cat. No. A190-114A, rabbit polyclonal antibody, Bethyl Laboratories, Montgomery, USA) was used to confirm that both rORF3p and rORF4p were produced as insoluble proteins in *E. coli*. The insoluble proteins were purified by repeated washes in BugBuster extraction reagent (EDM Millipore Corporation, San Diego, CA, US), then solubilized in 6 M urea. The denatured rORF3p and rORF4p (1.5 mg each) were used to immunize rabbits to induce production of the anti-rORF3p and anti-rORF4p antisera (Protein Purity, Isezaki, Japan).

2.8. Transformation of Magnaporthe oryzae

The isolate P2 was transformed with the hygromycin resistance (*hph*) gene and the enhanced green fluorescence protein (EGFP) gene as follows: The EGFP gene was amplified from the plasmid pMK412 (Watanabe et al., 2007) using primers designed to add *Eco*RI sites (Table S2). The PCR product was treated with T4 DNA polymerase (Takara Bio) in a 100 mM dNTP premix at 12 °C for 15 min, then the resultant fragment was inserted into the pAK2-Hyg-exp plasmid (Kato et al., 2012), which had been linearized using *Hpa*I. The construct was used to transform the spheroplasted P2 isolate, and the resultant transformants were selected on PDA plates with hygromycin B (200 mg/ml; Wako, Osaka, Japan). Transformants were confirmed by amplifying the *hph* gene using specific primers (Table S2) and by observation of EGFP using fluorescence microscopy (Olympus IX71; Tokyo, Japan; excitation 470–495 nm; emission 510–550 nm). To analyze the effect of MoCV1-D ORF4 on *M. oryzae*, the isolate Ina168 was transformed with pAK2-ORF4-MoCV1-D, or with an empty vector (pAK2-Hyg-exp).

2.9. Hyphal fusion

Virus infection via hyphal anastomosis was performed using the virus-infected original isolate APU10-199A as donor and the virus-free P2 isolate, transformed with the *hph* and EGFP genes, as recipient. Mycelial plugs of donor and recipient isolates were placed 2 cm apart on a 9 cm OMA plate supplemented with 0.75 mM $ZnSO_4$ (Ikeda et al., 2013), and incubated at 25 °C for 30 days. Several plugs picked up from the border between the two colonies were subcultured four times on OMA plates containing hygromycin B (200 μg/ml) to eliminate the donor cells.

2.10. Transfection of MoCV1-D virus particles

M. oryzae isolates P2 and the MoV2- and MoCV1-D-free APU10-199A were transfected with MoCV1-D virus particles via the protoplast-polyethylene glycol (PEG) method. Protoplasts of both recipient isolates were prepared as described in Aihara et al. (2018). MoCV1-D virus particles were purified from 5 g of frozen mycelia of APU10-199A cultured in a fermenter for 14 days by sucrose density gradient centrifugation as described above. Based on the transfection procedure by Ejmal et al. (2018), 130 μl of PEG 4000 was mixed with 70 μl of KTC buffer (1.8 M KCl, 150 mM Tris-HCl pH 8, 150 mM $CaCl_2$), 200 μl of purified viral suspension was added to the mixture. Additionally, 5 μl of 0.05 mM spermidine (Sigma-Aldrich, St. Louis, USA) and 200 μl of *M. oryzae* protoplast suspension were also added to the mixture. The mixture was agitated for 15 s, and placed on ice for 20 min 200 μl of PEG 400 and 100 μl of KTC buffer were added to the above mixture, gently agitated and placed on ice for 10 min. Then, 10 ml of STC-50 buffer (1.2 M sorbitol, 10 mM Tris-HCl pH 7.5, 50 mM $CaCl_2$) was added to the transfection suspension and gently mixed. After centrifugation at 5500 g for 15 min, the resultant pellet was resuspended in 2.5 ml of YG1/2S broth (0.5% yeast extract, 2% glucose, 0.6 M sorbitol, 25 mM $CaCl_2$) and incubated at room temperature for 4.5 h to regenerate protoplasts. Subsequently, the protoplast suspension was added to 50 ml of YG20SC medium (0.5% yeast extract, 2% glucose, 20% sucrose, 1% low melting agar), gently mixed and pour into 4 dishes (9 cm diameter) for further regeneration. After incubation at 26 °C for 4 or 5 days, individual colonies were transplanted to fresh PDA plates and then subcultured thrice every 6 days. To analyze whether the transfection was successful in isolated colonies, dsRNA was extracted as mentioned above and analyzed by RT-PCR with MoCV1 RdRp gene-specific primers as described previously (Komatsu et al., 2016).

2.11. Yeast transformation and growth assays

For heterologous expression of the MoCV1-D ORF4 in *Saccharomyces cerevisiae*, a full-length cDNA clone of the MoCV1-D ORF4 was obtained by RT-PCR using an ORF4-specific primer set (Table S2). The product was inserted into the *Bln*I/*Hpa*I sites of the pRST426 shuttle vector (Urayama et al., 2012) and the sequence integrity of the obtained clones was confirmed by Sanger sequencing with custom primers (Table S2). The *S. cerevisiae* strain W303-1A was transformed with the pRST426-DORF4 vector using the lithium acetate method (Gietz et al., 1995). Growth assays for yeast cells carrying pRST426-DORF4 or the empty pRST426 vector were performed as described by Okada et al., (2018).

2.12. Extraction and analysis of melanin biosynthesis-related intermediates

The extraction of melanin biosynthesis-related intermediates in *M. oryzae* was carried out as described previously with some modifications (Greenblatt and Wheeler, 1986; Wheeler and Greenblatt, 1988; Kurahashi et al., 1998). Spore and hyphae suspensions of MoCV1-D-

infected or -free isolates cultured on OMA media were spread on potato carrot dextrose agar plates and covered with single sheets of cellophane. After incubation at 26 °C in the dark for 7 days, 1 g of the fungal mat was scraped from the cellophane and pulverized in liquid nitrogen. The pulverized fungal powder was suspended in 30 ml of acetone and stirred for 30 min. The suspension was filtered through a filter paper, evaporated, and the residue was dissolved in a small amount of 20% CH_3CN in H_2O for HPLC analysis.

The extracts were analyzed using a LC-20A HPLC system (Shimadzu Co., Kyoto, Japan) under the following conditions: column, Kinetex XB-C18 (4.6 mm × 250 mm; Phenomenex Inc., Torrance, CA, USA); column temperature, 40 °C; mobile phase, linear gradient from 20% CH_3CN in H_2O/HCOOH (1000:1, v/v) to 80% CH_3CN in H_2O/HCOOH for 30 min; flow rate, 1.0 ml min^{-1}; UV detection, 334 nm.

Fractions separated at *Rt* 4.9 min and 8.5 min were analyzed by UPLC-time-of-flight mass spectrometry (UPLC-ToF/MS) (SYNAPT™ G2 HDMS™ coupled to ACQUITY UPLC® operated and analyzed by MassLynx software ver. 4.1, Nihon Waters K.K., Tokyo, Japan). The UPLC conditions were as follows: column, Kinetex C18 (2.1 mm × 100 mm; Phenomenex Inc., Torrance, CA, USA); column temperature, 40 °C; mobile phase, linear gradient from 10% CH_3CN in H_2O/HCOOH (1000:1, v/v) to 90% CH_3CN in H_2O/HCOOH for 10 min; flow rate, 0.4 ml min^{-1}; UV detection, photodiode array 200–400 nm. The mass analysis conditions were as follows: electrospray ionization; ionization, negative ion mode; analyzer, resolution mode (resolution: 20000); mass range (*m/z*), 100–1000.

3. Results

3.1. Detection of mycoviruses in a Japanese isolate of M. oryzae

We previously detected a MoCV1-related mycovirus by RT-PCR in a Japanese isolate of *M. oryzae*, named APU10-199A, which was collected in Akita prefecture in northern Japan. We obtained a partial sequence for the conserved region of the viral RdRp gene and found that it had a high level of nucleotide identity with those of MoCV1-A and MoCV1-B (Komatsu et al., 2016). To investigate the whole genome organization of this MoCV1-related virus, we purified its genomic dsRNAs from the APU10-199A isolate. In agarose (Fig. 1A) and polyacrylamide gels (Fig. S1), five distinct bands ranging from 2.6 to 3.6 kbp were tentatively named dsRNA1 to dsRNA5. We named the new MoCV1-related mycovirus MoCV1-D.

During subculturing or after freezing storage of the original APU10-199A isolate, we encountered a MoCV1-D derivative that had only four dsRNA segments, which corresponded to dsRNAs 1–4 (Fig. S2A). No amplification product was detected by RT-PCR using primers specific for the dsRNA5 of MoCV1-D (Fig. S2B, Table S2).

3.2. Sequence properties of the five MoCV1-D dsRNA segments and the 5.2 kbp-dsRNA in APU10-199A

We determined the complete nucleotide sequence of each dsRNA segment between 2.6 and 3.6 kbp in the APU10-199A isolate, using a series of full length cDNA clones. The sizes of the five dsRNA segments range from 2603 to 3557 nt, and these five dsRNAs were named dsRNA1 (the longest) to dsRNA5 (the shortest) (Fig. 2A). The sequences were registered in the DDBJ/EMBL/GenBank database with the following accession numbers: dsRNA1, LC432338; dsRNA2, LC432339; dsRNA3, LC432340; dsRNA4, LC432341; and dsRNA5, LC432342. As shown in Table 1, comparisons of the nucleotide sequences of MoCV1-D with those of MoCV1-A and MoCV1-B reveal moderately high levels of identities (72.2%–81.1%) for dsRNAs 1–4, but relatively low levels (63.6% and 63.5%) for dsRNA5 (Table 2).

The 5′-termini contain a highly conserved motif (5′-GCAAAAAAG AAUAAAGC-3′) (Fig. 2B), and this is also conserved among the other mycoviruses in cluster II of family *Chrysoviridae*, including MoCV1-A,

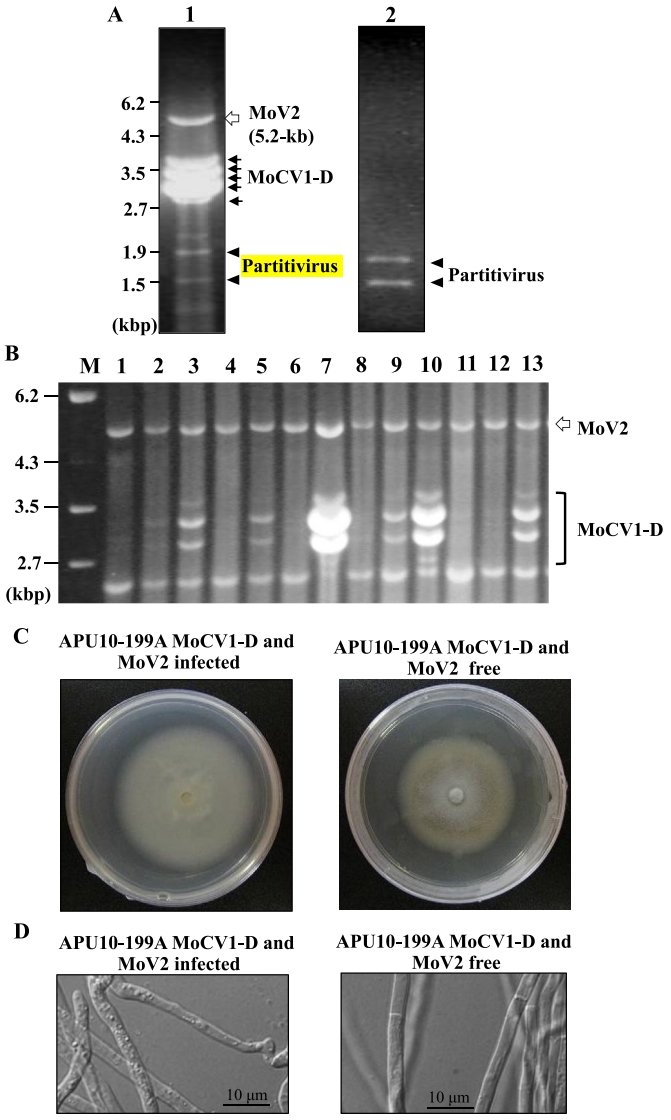

Fig. 1. Comparisons of dsRNAs, colony morphology, and hyphal morphology between the original APU10-199A isolate and a MoV2- and MoCV1-D-free isolate. (A) Migration patterns of dsRNAs isolated from APU10-199A (lane 1) and the MoV2 and MoCV1-D-free isolate (lane 2). The dsRNAs were electrophoresed in a 1% (w/v) agarose gel at 50 V for 4 h, stained with ethidium bromide, and visualized under UV. White arrow: the 5.2 kb dsRNA of MoV2. Black arrows: dsRNAs 1–5 of MoCV1-D. Arrowheads: dsRNAs of a partitivirus. (B) Agarose gel electrophoresis of dsRNAs in colonies grown from single conidia derived from APU10-199A (lanes 1–13). M: DNA marker (0.3 μg of λ DNA digested with EcoT14I). (C) Colonies grown on PDA medium at 26 °C for 10 days. (D) Hyphae cultured in YG liquid medium at 26 °C for 3 days, photographed under a light microscope (Olympus IX71; Tokyo, Japan) with differential interference contrast (DIC) optics.

MoCV1-B, AaCV1, Botryosphaeria dothidea chrysovirus 1 (BdCV1), Aspergillus mycovirus 1816 (AmV1816), FgV-Ch-9, and Tolypocladium cylinrosporum viruses 1 and 2 (TcV1 and 2).

Each MoCV1-D-dsRNA segment contains a single open reading frame (ORF). The predicted sizes of the encoded proteins are shown in Fig. 2A. A BLASTp analysis revealed that ORF1 encodes a member of the viral RdRp family. A phylogenetic analysis of a region of RdRp that contains 8 conserved motifs (Jiang and Ghabrial, 2004) showed that MoCV1-D belongs to the same clade as MoCV1-A and -B, within cluster II of the family *Chrysoviridae* (Fig. 3). BLASTp analyses revealed that the predicted amino acid sequences of ORFs 2, 3, and 4 show significant similarities to their counterparts in MoCV1-A and -B (82.5%–90.9%

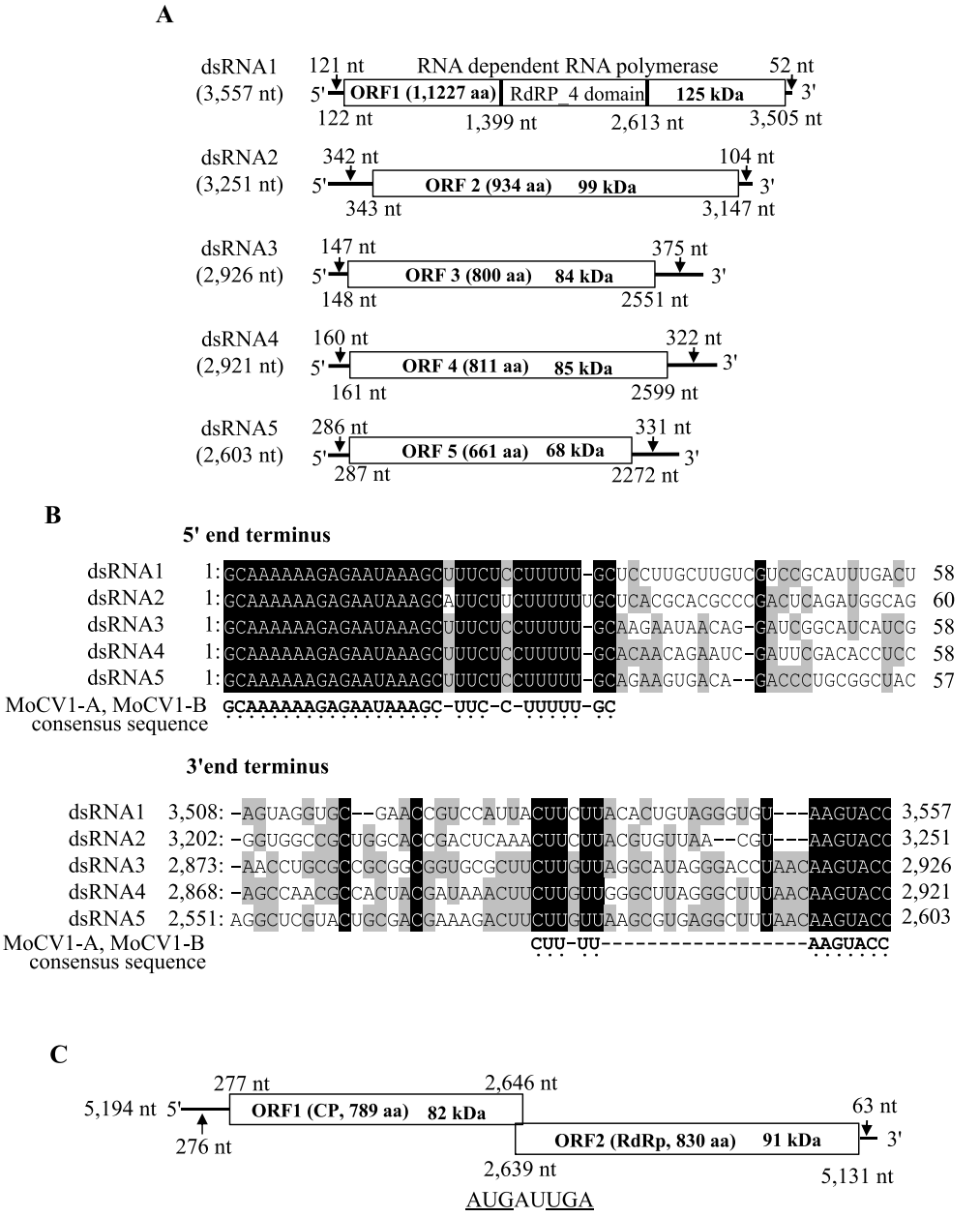

Fig. 2. Properties of the MoCV1-D and MoV2 genomes. (A) Genome organization of MoCV1-D. The total nucleotide length of each dsRNA is shown in parentheses below the name of the dsRNA. Open boxes denote ORFs. The predicted amino acid number and predicted molecular mass of each protein (kDa) is shown. Arrows indicate the 5′ and 3′ untranslated regions. (B) Multiple alignments of the 5′- and 3′-terminal regions of the coding strands of the five dsRNA segments of MoCV1-D. Black, 100% nucleotide identity; grey, 60–80% nucleotide identity. Sequences conserved between MoCV1-A and MoCV1-B are shown under each alignment. Dots show nucleotides conserved among all three MoCV1 strains. (C) Genome organization of MoV2. The viral genome is 5194 nt in length. Open boxes denote ORF1 and ORF2, respectively, with their predicted numbers of amino acids and molecular masses. The context of the overlapping region between the ORF1 terminal codon and the ORF2 initiation codon is shown under the diagram. CP: coat protein.

Table 1
Pairwise comparisons of nucleotide sequences between MoCV1-D and MoCV1-A or MoCV1-B.

MoCV1-DdsRNA segments	ViraldsRNA segments	Length(nt)	Identity(%)
dsRNA1 (3557 nt)	MoCV1-A dsRNA1	3554	81.1
	MoCV1-B dsRNA1	3558	81.0
dsRNA2 (3251 nt)	MoCV1-A dsRNA2	3250	78.9
	MoCV1-B dsRNA2	3254	77.5
dsRNA3 (2926 nt)	MoCV1-A dsRNA3	3074	75.8
	MoCV1-B dsRNA3	2874	72.2
dsRNA4 (2921 nt)	MoCV1-A dsRNA4	3043	76.0
	MoCV1-B dsRNA4	2997	73.9
dsRNA5 (2603 nt)	MoCV1-A dsRNA5	2879	63.6
	MoCV1-B dsRNA5	2880	63.5

identity) (Table 2). As expected, the ORF5-encoded protein of MoCV1-D exhibits lower sequence similarities with those of MoCV1-A and -B (70.3% and 65.9% identities, respectively). The proteins encoded by ORFs 1, 3, and 4 also show considerable homology with those of other viruses in Cluster II, while ORFs 2 and 5 show lower homology with those of other viruses (Table 2).

We also determined the nucleotide sequence of the 5.2 kbp dsRNA in APU10-199A (Fig. 1A, lane 1) by deep sequencing combined with the FLDS method, which allows the determination of full-length RNA virus sequences with high efficiency (Urayama et al., 2016b). The complete sequence of 5194 nt was deposited in the DDBJ/EMBL/GenBank database (accession no. LC432343). A BLASTx analysis revealed significant identity with the previously reported Magnaporthe oryzae virus 2 (MoV2), which was found in the *M. oryzae* isolate Ken 60-19 (AB300379) (Maejima et al., 2008). MoV2 is a member of the genus *Victorivirus*, family *Totiviridae*. ORF1 (nt 277–2646) encodes the coat protein and ORF2 (nt 2639–5131) encodes the RdRp (Fig. 2C). The termination codon of ORF1 overlaps the initiation codon of ORF2 in the octonucleotide sequence AUGAUUGA (nt 2639–2646). This feature differs from that of the MoV2 isolate from Ken 60-19, whose ORFs also overlap, but at the AUGA tetranucleotide, which is a typical “start and restart” motif conserved among the majority of victoriviruses (Ghabrial et al., 2013). The whole nucleotide identity between the MoV2 strains

Table 2
Pairwise comparisons of amino acid sequences between MoCV1-D and other chrysoviruses.

MoCV1-D ORFs	Viral ORFs	Length (aa)	Identity(%)	Similarity(%)
ORF1 (1127 aa)	MoCV1-A ORF1	1127	93.9	99.7
	MoCV1-B ORF1	1127	93.4	99.6
	TcV2 ORF1	1132	50.5	65.0
	WiV29 ORF1	916	52.8	67.1
	PjCV2 ORF1	1119	40.2	56.7
	AmV1816 ORF1	1084	38.8	55.4
	AaCV1 ORF1	1117	38.9	55.7
	BdCV1 ORF1	1116	38.7	54.9
	FodV1 ORF1	1139	34.2	51.1
ORF2 (934 aa)	MoCV1-A ORF2	934	83.7	88.3
	MoCV1-B ORF2	934	82.5	88.4
	BdCV1 ORF2	746	27.3	43.2
ORF3 (800 aa)	MoCV1-A ORF3	799	90.6	99.0
	MoCV1-B ORF3	784	88.8	97.7
	BdCV1 ORF3	717	32.9	46.8
	PjCV1 ORF3	687	33.6	48.6
	AaCV1 ORF3	774	31.4	47.0
	FodV1 ORF3	878	30.5	47.9
ORF4 (811 aa)	MoCV1-A ORF4	812	90.9	94.5
	MoCV1-B ORF4	811	89.2	92.6
	BdCV1 ORF4	768	27.4	44.8
	PjCV2 ORF4	783	28.9	46.1
	PjCV1 ORF4	770	26.3	42.1
	AaCV1 ORF4	771	26.5	41.4
	FodV1 ORF4	852	22.5	39.4
ORF5 (661 aa)	MoCV1-A ORF5	611	70.3	79.0
	MoCV1-B ORF5	666	65.9	74.4

from Ken 60-19 and APU10-199A is 98.0%, and the identities in the ORF1 and ORF2 sequences are 99.5 %and 99.8%, respectively.

Further analyses of other FLDS contigs revealed that two contigs of 1201 bp and 705 bp showed significant homology with the RdRp (KX119172) and coat protein (KX119173) genes of Magnapothe oryzae partitivirus 1, respectively. Together, our data indicate that the original APU10-199A isolate was co-infected by three virus species belonging to the families *Chrysoviridae, Totiviridae*, and *Partitiviridae*.

3.3. MoCV1-D contributes to the phenotypes of the M. oryzae isolate APU10-199A

To analyze the effects of MoCV1-D infection on the phenotype of the host fungus, we isolated single conidia of APU10-199A and examined the resultant colonies for the presence of the dsRNAs of MoCV1-D, MoV2, and the partitiviruses. Among the 74 colonies grown from single conidia, the dsRNA bands of MoV2 (5.2 kbp) and a partitivirus (1.5–2.0 kbp) were generally stably maintained in the host fungus. In contrast, the intensities of the MoCV1-D dsRNA bands were remarkably variable and showed inconstant patterns (Fig. 1B, lanes 1–13). Such significant quantitative variation was also observed in AaCV1, which is also in cluster II of the *Chrysoviridae* (Okada et al., 2018). Two of the isolates had completely lost both MoCV1-D and MoV2, but still kept the 1.5–2.0 kbp-dsRNAs of a partitivirus, and several other colonies had lost only MoCV1-D (Fig. 1 and Fig. S3). We used RT-PCR to confirm the absence of MoCV1-D or of both MoCV1-D and MoV2 (Figs. S3B and C). The original isolate, APU10-199A, exhibited impaired growth on PDA plates, with abnormal pigmentation, albino mycelia, and reduced aerial hyphae formation when compared with the MoCV1-D- and MoV2-free

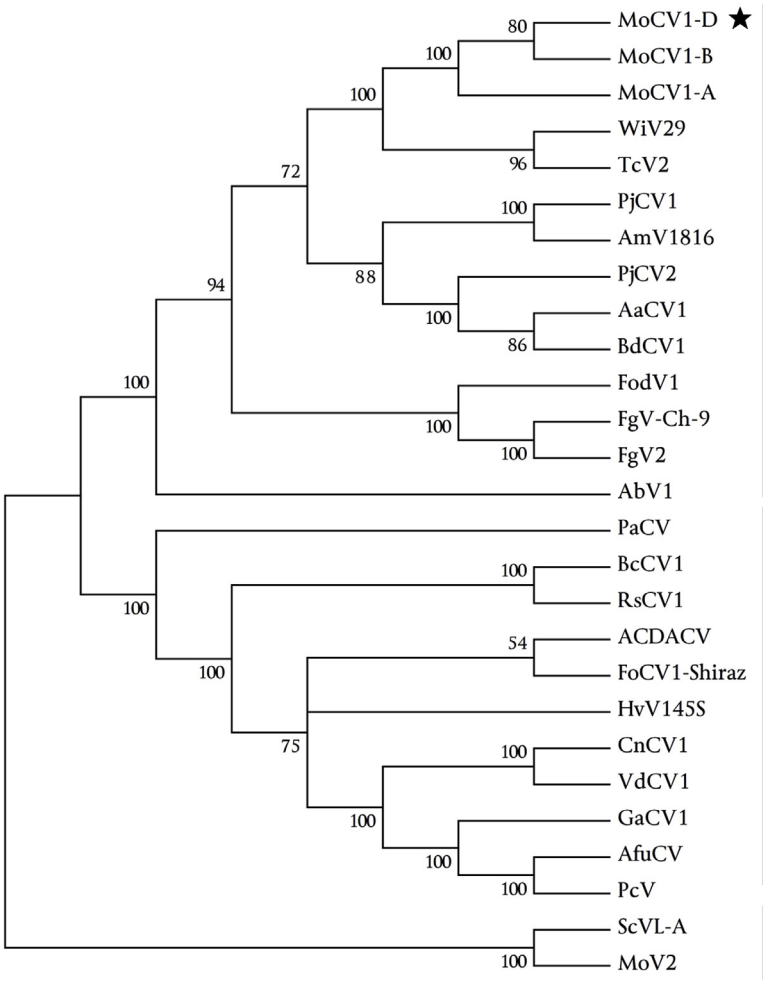

Fig. 3. Phylogenetic analysis of the family *Chrysoviridae*, based on the RdRp core region. The evolutionary history was inferred by using the Maximum Likelihood method based on the Le_Gascuel_2008 model. An evolutionary analysis was conducted in MEGA7 software (Kumar et al., 2016). Numbers at nodes represent bootstrap values as percentages estimated from 1000 replicates. A substitution model for this phylogenetic analysis was applied based on an LG model. A discrete Gamma distribution was used to model evolutionary rate differences among sites (5 categories (+G, parameter = 2.8574)). The rate variation model allowed for some sites to be evolutionarily invariable ([+I], 1.91% sites). Abbreviations of virus names and accession numbers of their RdRp genes are provided in Supplementary Table S1. *Saccharomyces cerevisiae* virus L-A (ScVL-A) and Magnaporthe oryzae virus 2 (MoV2), which are classified in the family *Totiviridae*, were used as a outgroup. The black star indicates MoCV1-D, which was analyzed in this study.

isolate (Fig. 1C and Fig. S3A). Abnormal morphology, such as enlarged vesicles, was frequently observed in the original APU10-199A isolate, while this was rarely observed in the MoCV1-D- and MoV2-free isolate (Fig. 1D). These phenotypes were similar to those of the MoCV1-B-infected *M. oryzae* isolate S-0412-II 2a (Urayama et al., 2014a), except that S-0412-II 2a exhibited an increased number of branches and a lack of polarity, and this was less pronounced in APU10-199A (Fig. 1D and Fig. S3D). The MoCV1-D-free isolate that was still infected with MoV2 showed restored growth phenotypes, such as normal hyphae and uniform pigmentation (Figs. S3A and D), and this suggested that MoCV1-D was the most influential agent leading to the impaired growth of APU10-199A. However, it cannot be ruled out that virus/virus interactions may have had some effect on the phenotype of APU10-199A. In the white root rot fungal strain W8, co-infection with the partitivirus RnPV1 was required for the hypovirulence conferred by the megabirnavirus RnMBV2 (Sasaki et al., 2016).

3.4. Virus particles containing dsRNAs and multiform structural proteins

To determine whether the dsRNAs in the isolate APU10-199A were associated with virus particles, we attempted to purify viral particles from a 10-day jar-fermenter culture, using standard methods without chloroform/butanol (Urayama et al., 2010; Okada et al., 2018). The purified viral fractions were investigated for the presence of the MoCV1-D and MoV2 dsRNAs by agarose gel electrophoresis (Fig. 4A). Based on this dsRNA profile, we determined that the buoyant densities in CsCl ranged from approximately 1.35–1.39 g cm^{-3} for MoCV1-D (Fig. 4A, lanes 3 to 6, Pool I), and 1.41–1.49 g cm^{-3} for MoV2 (lanes 7 to 10, Pool II). When we examined Pools I and II by transmission electron microscopy, we observed isometric virus particles with diameters of about 35 nm in Pool I and about 38 nm in Pool II (Fig. 4B). Although there may have been some mixing of MoCV1-D particles in the Pool II fractions, or vice versa, these results suggest that MoCV1-D and MoV2 were mostly separated into two viral fractions in the CsCl density gradient.

SDS-PAGE of the purified virions in Pool I revealed multiple distinct protein bands of 120, 66, 60, 58, and 53 kDa (Fig. 4C, Pool I). Anti-MoCV1-A serum was used for western blot analysis because the amino acid sequences of the viral structural proteins encoded by dsRNA3 and dsRNA4 were highly conserved between MoCV1-A and MoCV1-D (see Table 2). Since MoCV1-A was the only virus infecting the S-0412-II 1a isolate (Urayama et al., 2010), the anti-MoCV1-A serum was considered to be suitable for detecting only MoCV1-D proteins. Indeed, the antiserum detected the 120, 66, 60, and 58 kDa proteins (Fig. 4D), indicating that these four protein bands represented viral structural proteins of MoCV1-D. Based on the predicted molecular mass, the 120 kDa band was likely to be the RdRp encoded by ORF1, consistent with our previous results for MoCV1-A (Urayama et al., 2012). The Pool II fractions contained three additional bands of 90, 79, and 72 kDa, and these were not detected by the anti-MoCV1-A antiserum (Fig. 4C and D). Therefore, we concluded that these were the viral structural proteins of MoV2.

We found previously that the size patterns of viral structural proteins differed between short-term and long-term cultures of the infected cells. When fresh mycelia from a 3-day jar-fermenter culture were used as materials for viral particle purification, we detected proteins of approximately 120, 95, and 85 kDa in the CsCl density range 1.35–1.39 g cm^{-3} (Pool I) (Fig. 4E). These roughly corresponded to the predicted full-sized proteins encoded by ORFs 1, 3, and 4 (see Fig. 2A). In addition, we detected putative partial degradation products of approximately 71, 66, and 60 kDa (Fig. 4E). The antiserum against MoCV1-A particles also detected the full-sized structural proteins of MoCV1-D (Fig. 4F), and this supports the idea that the 71, 66, and 60 kDa proteins in the Pool I fractions (Fig. 4C, E, and 4F) were partially degraded products of the full-sized ORF3 and/or ORF4 proteins.

The ORF3 and ORF4 proteins were predicted to be the major structural proteins of MoCV1-D due to their abundance. To investigate the ORF3 and ORF4 proteins further, we produced recombinant versions of the proteins in *E. coli* and then raised antisera against the recombinant proteins (Fig, S5A, S5B). In the following viral purification experiments, we skipped the CsCl centrifugation step because we had realized that the sucrose gradient step was sufficient to yield similar patterns of partially degraded products. We used 3-day and 14-day mycelium cultures and recovered the virus-rich fractions from the sucrose gradients, then performed SDS-PAGE (Fig. 4G) and western blot analyses (Fig. 4H, I, and 4J) of the viral proteins. The main bands in SDS gels containing proteins from the 3-day and 14-day cultures were 95 and 60 kDa, respectively, and each culture also produced other minor bands (Fig. 4G, lanes 2 and 3). The anti-MoCV1-D ORF3 antiserum detected mainly bands of 85 kDa and 60 kDa in the 3-day and 14-day cultures, respectively, along with other minor bands (Fig. 4H, lanes 2 and 3). Since this antiserum detected no signal in similarly prepared protein fractions from an isolate that was free of both MoCV1-D and MoV2 (Fig. 4H, lane 1), all of the detected bands in Fig. 4H were derived from the MoCV1-D ORF3 protein and not from host cellular components.

An antiserum raised against the MoCV1-A ORF3 C-terminal peptide (CSSDGASGGSRGEEL) detected only the 85 kDa structural protein in the 14-day cultured mycelia (Fig. 4I, lane 3). In proteins from the 3-day culture, this antiserum detected proteins of 95, 92, and 88 kDa and a ladder of smaller degraded products (Fig. 4I, lane 2). The anti-MoCV1-D ORF4 antiserum detected mainly bands of 85, 75, and 70 kDa among proteins from the 3-day culture (Fig. 4J, lane 2), and bands of 66, 60, and 58 kDa among proteins from the 14-day culture (Fig. 4J, lane 3). We also found that short-term culture of the host fungus in a jar-fermenter allowed us to detect undegraded and intermediate forms of the structural proteins.

3.5. Horizontal transmission of MoCV1-D via hyphal fusion

We used hyphal fusion to introduce MoCV1-D or MoV2 into a virus-free rice-pathogenic *M. oryzae* isolate named P2 (Kamakura et al., 2002), which we first transformed with a bacterial hygromycin-resistant (*hph*) gene (Fig. 5A). P2 and APU10-199A were dual-cultured on the same OMA plate supplemented with 0.75 mM $ZnSO_4$ to suppress apoptosis caused by vegetative incompatibility (Ikeda et al., 2013) and promote hyphal fusion (Fig. S6A). After four successive subcultures on medium containing hygromycin, mycelia were cultured in YG liquid medium and surveyed for the presence of viral dsRNA bands. Finally, we obtained two strains that contained four dsRNAs ranging from 2.8 to 3.6 kbp (Fig. 5B, lanes 3 and 4). We analyzed these strains by PCR using *hph*-specific primers and a primer specific for a terminal inverted repeat (Pot2-TIR; Table S2). The strains carried the *hph* gene (Fig. S6B) and showed a pattern of polymorphic repetitive DNA that was identical to that of P2 (Fig. S6C), indicating that the sub-cultured mycelia were derived from P2. RT-PCR analysis with primers specific to the MoCV1-D dsRNA1 detected an amplicon of the expected size (Fig. 5C, lane 3), demonstrating that MoCV1-D was transmitted from APU10-199A to P2 via anastomosis. Interestingly, the recipient isolate did not contain the MoCV1-D dsRNA5, based on dsRNA electrophoresis (Fig. 5B, lanes 3 and 4) and RT-PCR with dsRNA5-specific primers (data not shown). We also did not detect the MoV2 dsRNA in dsRNA gels or by RT-PCR (Fig. 5B and D). This suggests that MoV2 is less readily transmitted by hyphal fusion than MoCV1-D.

To confirm that the P2 isolates containing MoCV1-D dsRNAs also contained virions, we purified virus particles from one of the isolates as described above. The CBB-stained band-pattern of isolated proteins was very similar to that of MoCV1-D purified from APU10-199A (Fig. 5E, and the P2 isolate also contained virions with similar morphology to those purified from the APU10-199A (Fig. 5F).

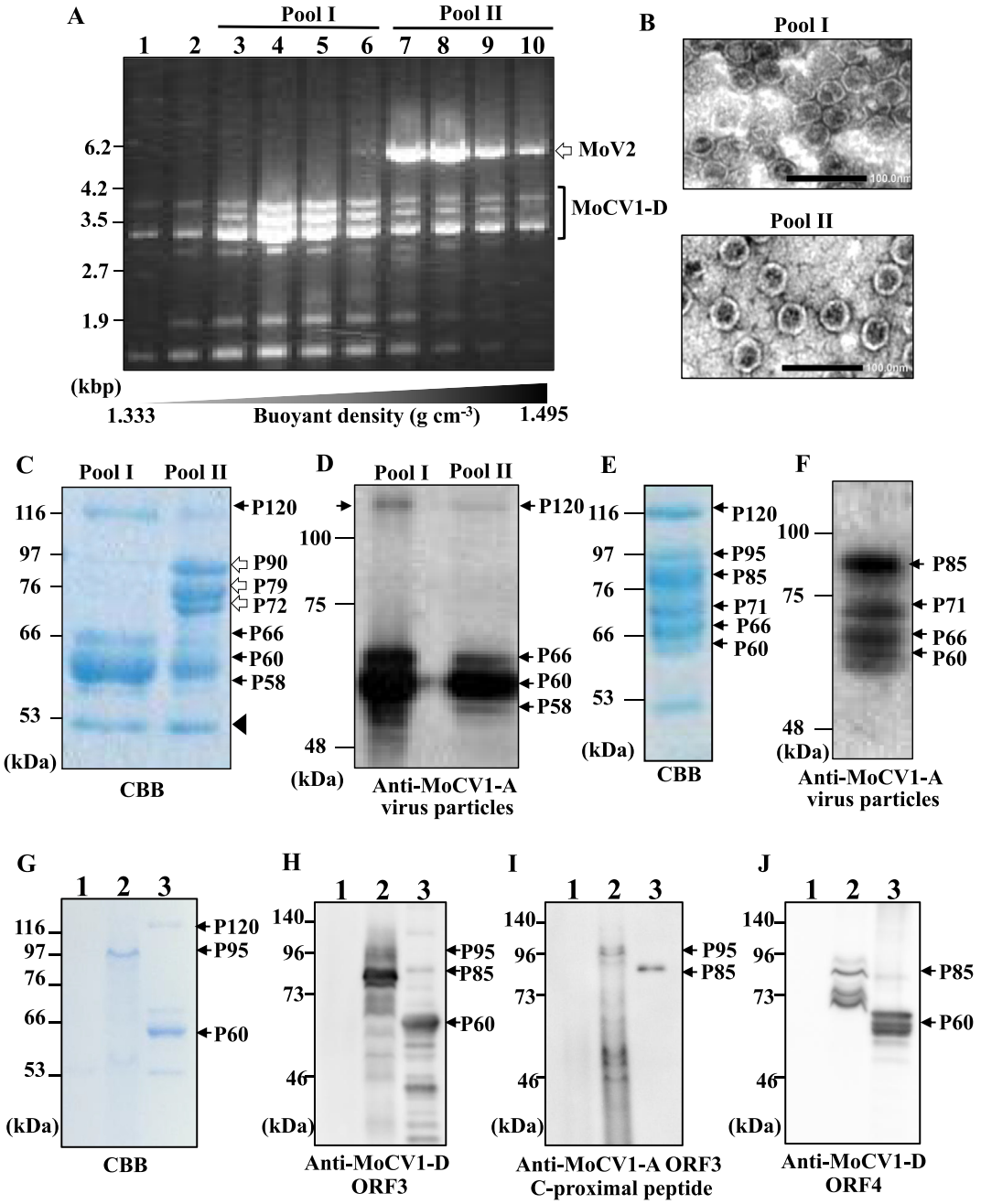

Fig. 4. Purification of virus-like particles from isolate APU10-199A. The particles were purified from fresh mycelia of the fungus, cultured in a fermenter for 10 days (A–D) or 3 days (E, F). (A) Agarose gel electrophoresis of the total nucleic acids extracted from each fraction after CsCl density equilibrium centrifugation. Pool I (lanes 3–6) and Pool II (lanes 7–10) are the fractions used for further analyses. White arrow: the 5.2 kbp dsRNA of MoV2. Bracket: dsRNAs 1–5 of MoCV1-D. (B) Negative contrast electron micrograph of the uranyl acetate-stained virus particles in Pool I (upper panel) and Pool II (lower panel). The scale bars indicate 100 nm. (C–F) SDS-PAGE and western blot analyses of viral structural proteins. Whole proteins were separated by 8% SDS-PAGE and stained with CBB (C, E) or immunoblotted with antiserum against MoCV1-A virus particles (D, F). Black arrows, white arrows, and the arrowhead indicate predicted structural proteins of MoCV1-D, MoV2, and a partitivirus, respectively. (G–J) Analysis of viral structural proteins purified from the MoCV1-D- and MoV2-free strain cultured in a fermenter for 3 days (lane 1), and from the original isolate APU10-199A cultured in a fermenter for 3 days (lane 2) or 14 days (lane 3). (G) SDS-PAGE stained with CBB. (H–J) Western blot analyses with antisera against the MoCV1-D ORF3 protein (H), the MoCV1-A ORF3 C-proximal peptide (I), and the MoCV1-D ORF4 protein (J).

3.6. Transfection of M. oryzae protoplast with MoCV1-D virus particles

To further evaluate our chrysovirus infection system in *M. oryzae* chrysovirus, we attempted to introduce purified MoCV1-D virus particles into protoplasts of P2 and MoV2- and MoCV1-D-free APU10-199A isolates. RT-PCR analyses with MoCV1 RdRp gene-specific primers resulted in the detection of specific amplicon in almost all regenerated colonies of both recipient isolates (Fig. S7). Therefore, the protoplast-PEG method is effective in the transfection of *M. oryzae* by MoCV1-D chrysovirus.

3.7. Heterologous expression of ORF4 caused growth inhibition of the yeast S. cerevisiae

Previously, we showed that heterologous expression of MoCV1-A *ORF4* induced cytological damage to the yeasts *S. cerevisiae* (Urayama et al., 2012) and *C. neoformans* (Urayama et al., 2014b). To investigate the effect of MoCV1-D *ORF4* in yeast cells, we transformed yeast with a

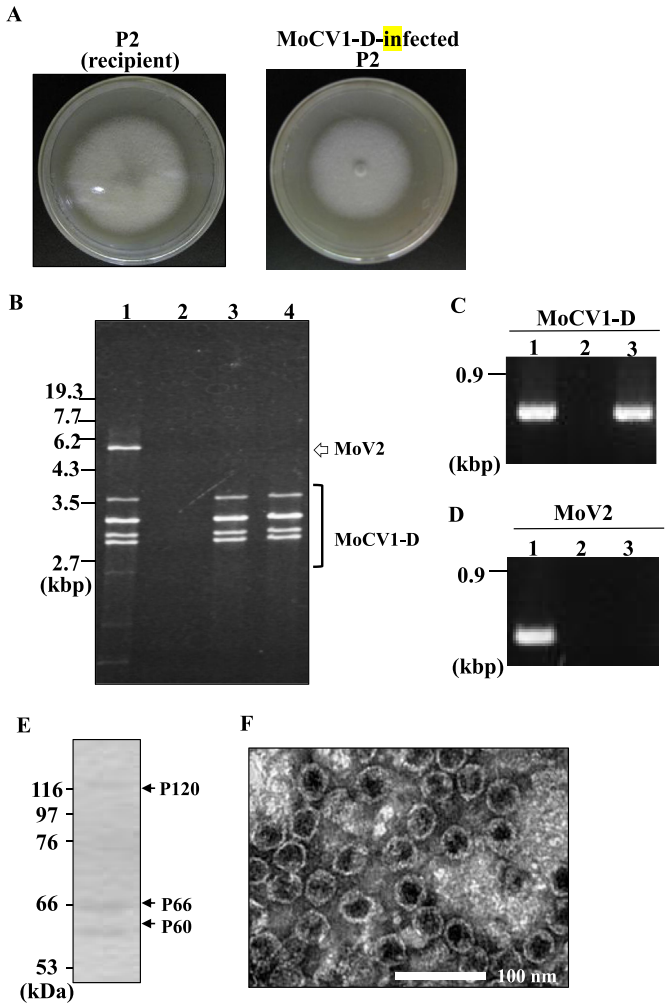

Fig. 5. Transmission of MoCV1-D from the donor isolate APU10-199A to the virus-free recipient isolate P2. (A) Colony morphologies of the virus-free P2 isolate and a MoCV1-D-infected P2 isolate after hyphal fusion and selection. Each isolate was incubated for 10 days at 25 °C on an OMA plate. (B) Migration patterns of purified dsRNAs from APU10-199A (lane 1), the virus-free P2 (lane 2), and two infected P2 isolates after hyphal fusion and selection (lanes 3 and 4). Electrophoresis was performed in 5% (w/v) polyacrylamide gels. (C, D) Detection of the MoCV1-D RdRp gene (C) and MoV2 (D) by RT-PCR using MoCV1-D dsRNA1 or MoV2 dsRNA specific primers (see Table S2). Purified dsRNAs derived from the donor (lane 1), the recipient (lane 2) and an infected progeny isolate (lane 3) were used as templates. (E) Analysis of viral structural proteins in the infected P2 isolate after purification in a sucrose density gradient. The 8% SDS-polyacrylamide gel was stained with CBB. (F) Negative contrast electron micrograph of 2% uranyl acetate-stained virus particles in the purified fraction.

high-expression vector carrying *ORF4*, and monitored cell growth at 30 °C by measuring the turbidity (OD_{600}) of the liquid culture every 3 h, and performing viable cell counts every 6 h. The MoCV1-D *ORF4* transformants showed decreases in OD_{600} values (Fig. 6A) and viable cell numbers (Fig. 6B) when compared with the control vector transformants. The viable cell numbers of the *ORF4* transformants remained at about half of those of the controls throughout the experiment. When the cells were grown at 35 °C rather than at 30 °C, the differences in turbidity and viable cell counts was more pronounced (Fig. S8). In addition, by using differential interference contrast microscopy, we observed severe cytological damage, such as accumulation of enlarged vacuoles and non-uniform cell morphology, in MoCV1-D *ORF4* transformants compared with control vector transformants (Fig. 6C and D). These results indicated that expression of MoCV1-D *ORF4* resulted in growth inhibition of *S. cerevisiae*.

Consistent with these results, when we transformed MoCV1-D ORF4 gene into *M. oryzae* (strain Ina168) and established the fungal isolate constitutively expressing MoCV1-D ORF4, we observed abnormal shaped hyphae with enlarged vacuoles. This is similar to the abnormal hyphal phenotype of the MoCV1-A- and MoCV1-B-infected *M. oryzae* (Urayama et al., 2010, 2014a) (Fig. S9).

3.8. Release of MoCV1-D and MoV2 from mycelia into the culture supernatant

We previously found that MoCV1-A was released from the mycelia of virus-infected *M. oryzae* into the culture supernatant (Urayama et al., 2010). To investigate whether MoCV1-D is released into the culture medium, we cultured APU10-199A in liquid medium and collected the supernatant over 2–8 weeks. The dsRNAs of both MoCV1-D and MoV2 were detected after 4 weeks of culture, and their combined concentration peaked at 7 weeks, with about 300 ng dsRNA per 250 µl of culture supernatant (Fig. 7A). MoV2 was detected earlier than MoCV1-D. We also detected the viral dsRNAs in the precipitate of a 15-day jar fermenter culture supernatant (Fig. 7B), indicating that these dsRNAs were released from the mycelia under two different culture conditions. However, western blot analyses of the suspensions with anti-MoCV1-D ORF3 antiserum (Fig. 7C), anti-MoCV1-D ORF4 antiserum (Fig. 7D), or anti-MoCV1-A virus particle antiserum (Fig. S10) revealed weak and smeared protein bands that were unlike the bands obtained when virions were purified from mycelia (see Fig. 4H and J).

3.9. Qualitative differences in melanin biosynthesis-related intermediate accumulation between MoCV1-D-infected and MoCV1-D-free isolates

As shown in Fig. 1 and Fig. S3, MoCV1-D infection of *M. oryzae* resulted in impaired phenotypes including abnormal pigmentation and colony albinization. It was assumed that these phenotypic changes were caused by inhibition of melanin biosynthesis in the host fungus. Therefore, we examined the accumulation of melanin biosynthesis-related intermediates in MoCV1-D-free and -infected isolates by HPLC and UPLC-ToF/MS. When an extract prepared from the MoCV1-D-free isolate was directly subjected to HPLC analysis as described in the Materials and Methods, some compounds with UV absorption at 334 nm (a highly selective wavelength) were detected as representative peaks 1 and 2 at *Rt* 4.9 min and 8.5 min, respectively (Fig. 8A). However, apart from two small peaks at *Rt* 13.0 min and 13.4 min, no significant peaks were observed in the extract from the MoCV1-D-infected isolate (Fig. 8B). To confirm the production of melanin biosynthesis-related intermediates, the fractions separated at *Rt* 4.9 min and 8.5 min were further subjected to UPLC-ToF/MS analysis. Two main ions were identified in the *Rt* 4.9 min fraction from the MoCV1-D-free isolate. Mass spectra and the following elemental composition analyses confirmed that the ion at *m/z* 193.0503 $[M–H]^-$ had the chemical formula $C_{10}H_9O_4$, which is a deprotonation compound of scytalone that is a known intermediate in melanin biosynthesis. The ion at *m/z* 175.0390 $[M–H–H_2O]^-$ had the formula $C_{10}H_7O_3$, which is the same compound in dehydrated form (Fig. 8C). In contrast, there were no mass spectra corresponding to these intermediates in the of MoCV1-D-infected isolate (Fig. 8D). The *Rt* 8.5 min fractions from both isolates also did not contain any melanin biosynthesis-related intermediates (data not shown). These data suggest that the loss of scytalone production in the MoCV1-D-infected isolate is responsible for its abnormal pigmentation and colony albinization.

4. Discussion

In many aspects, the dsRNA genome and virion of MoCV1-D from the Japanese *M. oryzae* isolate APU10-199A are similar to those of MoCV1-A and MoCV1-B, which were found in Vietnamese isolates of *M.*

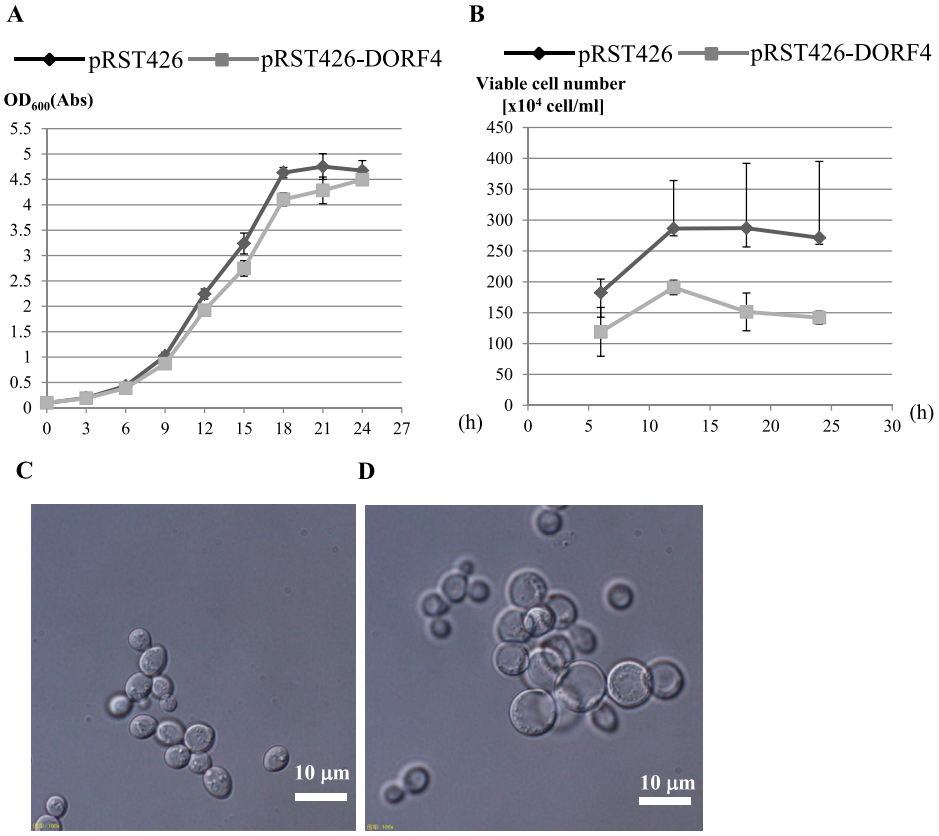

Fig. 6. Heterologous expression of MoCV1-D ORF4 in *S. cerevisiae* cells grown at 30 °C. (A, B) Growth curves of cells transformed with pRST426-DORF4 and the empty vector pRST426. (A) Time-course of the optical densities at 600 nm measured every 3 h. (B) Time-course of viable cell numbers measured every 6 h. Data are means ± standard error for three independent colonies. (C, D) Morphologies of cells transformed with the empty vector (C) or with pRST426-DORF4 (D) after 18 h of culture at 30 °C. Cells were examined with by light microscopy with DIC optics.

oryzae. The MoCV1-A dsRNA3 (AB560763) and dsRNA4 (AB560764) carry adenine-rich sequences of about 130 and 100 bp, respectively, interrupted by other nucleotides, near their 3′-terminal regions (Urayama et al., 2010). However, similar sequences were not found near the 3′ termini of the MoCV1-D dsRNA3 or dsRNA4, nor were they found in the MoCV1-B dsRNA3 (AB824669) or dsRNA4 (AB824670) (Urayama et al., 2014a). An important difference between MoCV1-D and the Vietnamese strains is in the dsRNA5 segment. Compared with the other dsRNA segments, the dsRNA5 of MoCV1-D is smaller than, and has lower sequence identity with, the dsRNA5 segments of MoCV1-A and MoCV1-B (Table 1). Furthermore, the dsRNA5 of MoCV1-D appears to be dispensable for viral propagation, since fungal isolates lacking dsRNA5 arose naturally during subculturing. This was also the case for MoCV1-B but not MoCV1-A. The causes of these differences are unknown, but the dsRNA5 segment could be conditionally beneficial for viral propagation. Recently, we identified several more Japanese *M. oryzae* isolates which were also infected with MoCV1-D. Their dsRNA5 segments also showed lower identities (64%) with those of MoCV1-A and MoCV1-B, but high identities (over 98%) with those of other MoCV1-Ds. AaCV1, which infects a Japanese pear pathotype of *Alternaria alternata*, is another chrysovirus that can lose a dsRNA segment during serial passages (Okada et al., 2018). MoCV1-D and AaCV1 show considerable homologies and similarities between ORFs in most segments (Table 2), however, the dsRNA5 of AaCV1 is about 2 kbp smaller and shows no significant sequence similarity with the dsRNA5 of MoCV1-D. These results suggested that the dsRNA5 segments of chrysoviruses in cluster II, which possess conserved 5′- and 3′-termini, are conditionally dispensable for virus propagation but may have some function for propagation in agricultural environments.

Recently, a rice blast fungus doubly infected with the victorivirus MoV3 and a chrysovirus MoCV1-C was reported in the Hubei province of China (Tang et al., 2015). No sequence data were reported for MoCV1-C, but the coat protein amino acid sequences of MoV2 found in APU10-199A and MoV3 found in the Chinese *M. oryzae* isolate containing MoCV1-C showed 67% identity (Tang et al., 2015). Based on these observations we assumed that the Chinese and Japanese strains are distinct, and that MoCV1-D is a new strain of MoCV1 with unique properties.

We isolated single conidia from APU10-199A and obtained isolates that lacked MoCV1-D or MoCV1-D and MoV2. The loss of MoCV1-D (with or without MoV2) restored normal colony and hyphal morphologies, indicating that like MoCV1-A and -B, MoCV1-D confers growth inhibition on the host fungus. However, it is not always the case that chrysoviruses, but not victoriviruses, affect the host fungus phenotypes. Mixed infection of *H. victoriae* by the victorivirus HvV190S and the cluster I chrysovirus HvV145S causes diseased phenotypes in the host fungus. Although no fungal isolate has been found that is solely infected by Hv145S, DNA transformation and transfection assays strongly suggest that the disease phenotypes are caused by HvV190S, and that HvV145S does not to affect colony morphology (Xie et al., 2016).

Heterologous expression of the MoCV1-A and -D ORF4 proteins significantly reduced the growth of *S. cerevisiae* and induced cytological damage in yeast cells (Fig. 6 and Urayama et al., 2016a). Expression of a structural protein of FgV-Ch-9 reduced transcription of a gene encoding a symptom alleviation factor, leading to virus-infection-like symptoms in *Fusarium graminearum* (Bormann et al., 2018). These results suggest that the chrysoviruses proteins corresponding to the MoCV1-A and -D ORF4 protein are generally involved in host fungal attenuation.

Like MoCV1-A (Urayama et al., 2012) and MoCV1-B (Urayama et al., 2014a), the viral structural proteins of MoCV1-D are partially degraded after long term jar-culture (10–14 days). Western blot analyses with anti-ORF3 and anti-ORF4 antisera clarified that these proteins (both about 85 kDa) are the major components of the MoCV1-D particles, and are partially reduced to proteins of about 60 kDa after long-term culture. Since nutrition sources are gradually depleted during long-term culture, we speculate that changing the capsid morphology from the full-sized particles (85 kDa) to the “core” particles (60 kDa) is

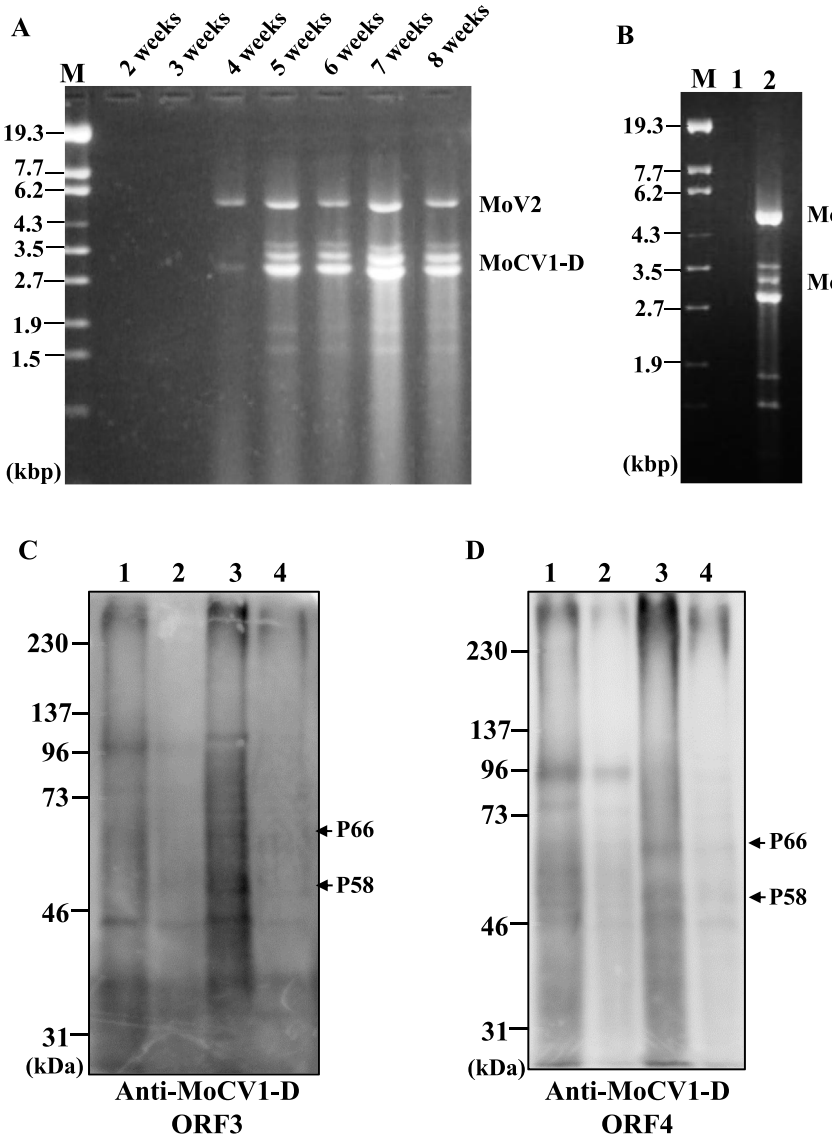

Fig. 7. The dsRNAs of MoCV1-D and MoV2 were released into culture supernatants during long-term cultivation of the mycovirus-infected *M. oryzae* isolate APU10-199A. (A) Supernatants (250 µl) were harvested from liquid flask cultures after 2–8 weeks of cultivation, and the extracted nucleic acids were electrophoresed in a 1% agarose gel. M: DNA marker (0.3 µg of λ DNA digested with *Eco*T14I). (B–D) Jar-fermenter cultures were grown for 15 days, and then the culture supernatants were centrifuged at 17,000 × *g*, 15 min to remove cell debris. The resulting supernatants were ultra-centrifuged at 148,000 × *g*, 3 h and the precipitates were suspended in 800 µl of 0.1 M phosphate buffer, pH 8.0. (B) Total nucleic acids were extracted from the 50 µl of suspension and electrophoresed in 1% agarose gels. Lanes: M, DNA marker; 1, the MoCV1-D- and MoV2-free isolate derived from APU10-199A; 2, the original isolate APU10-199A. (C, D) Western blot analyses using antisera against the MoCV1-D ORF3 protein (C) and the MoCV1-D ORF4 protein (D). Lanes: 1 and 2, the MoCV1-D- and MoV2-free isolate; 3 and 4, the original isolate; 2 and 4; samples were diluted 5-fold. Black arrows indicate the predicted MoCV1-D structural proteins.

advantageous for persistent viral infection of the nutrient-limited host fungi. This implies that the structural proteins of MoCV1-D have at least two different phases, depending on the nutritional status of the host fungus. However, it is also possible that protease activities are enhanced as cultures get older, causing degradation of the CPs during particle purification.

The MoCV1-D ORF3 antiserum detected many smaller ladder-like signals as well as the main signals from bands of about 85 kDa (3-day culture) or 60 kDa (14-day culture) (Fig. 4H). This suggested that the ORF3 protein tends to be degraded randomly rather than by some controlled process. On the other hand, the ORF4 protein tended to be degraded into regular-sized products of 85, 71, and 68 kDa (3-day culture) or 66, 60, and 58 kDa (14-day culture) (Fig. 4J). Such regulated processing may confer biological functions on each partially degraded protein. Indeed, we previously demonstrated that the central region of the MoCV1-A ORF4 protein (325–575 aa, designated as the SUa region) is partially conserved among cluster II mycoviruses and severely inhibits the growth of yeast cells when overexpressed in the cells (Urayama et al., 2016a).

It was also notable that a protein of approximately 95 kDa was detected after CBB staining and western blot analyses with the anti-MoCV1-D ORF3 and anti-MoCV1-A ORF3 C-proximal peptide antisera (Fig. 4G–I, lanes 2). The predicted molecular mass of the ORF3 protein is 84 kDa. We previously reported that the MoCV1-A ORF4 is expressed as a 100 kDa protein in *Pichia pastoris*, whereas the expected full-sized ORF4 protein is 85 kDa. We concluded that the MoCV1-A ORF4 protein may be glycosylated (Urayama et al., 2016a). Although we have not expressed the ORF3 protein in *P. pastoris*, our results suggest that the MoCV1-D ORF3 protein might also undergo post-translational modification, such as glycosylation or phosphorylation, even when expressed in *M. oryzae*. Intriguingly, the anti-MoCV1-A ORF3 C-proximal peptide antiserum mainly recognized the 85 kDa protein in extracts from the long-term culture (Fig. 4I, lane 3), whereas several degraded protein bands were detected in addition to the 95 kDa protein after short-term culture (lane 2). Possibly, the C-terminal amino acid sequences of the MoCV1-D ORF3 are easily degraded by carboxyl peptidases.

Although the mechanisms by which the MoCV1s are released outside cells are still unknown, this release phenomenon is characteristic of MoCV1 since it is observed in MoCV1-A and MoCV1-B (Urayama et al., 2010; Urayama et al., 2014a) as well as MoCV1-D. The MoCV1-D dsRNA concentrations in the culture supernatant reached approximately 1 µg/ml (Fig. 7A). However, the signals of the viral proteins in western blot analyses were relatively weak, suggesting that the viral structural proteins are fragile outside the cell. It is possible that the MoCV1-D and MoV2 dsRNAs were no longer packaged in solid protein

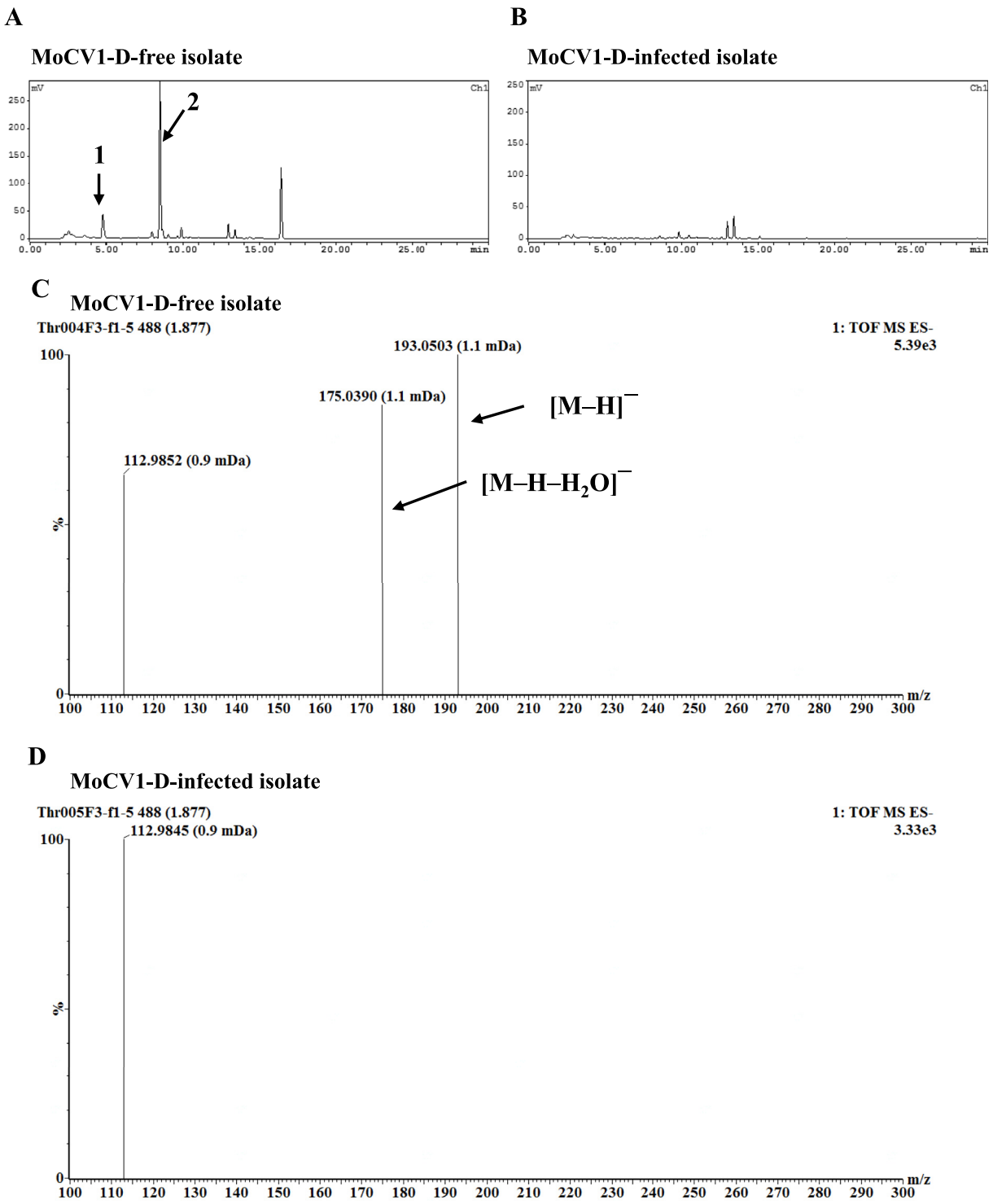

Fig. 8. Qualitative analyses of melanin biosynthesis-related intermediates in MoCV1-D-free and MoCV1-infected isolates. (A, B) HPLC chromatograms of extracts from MoCV1-D-free (A) and MoCV1-D-infected (B) isolates. (C, D) Accurate mass spectra in fractions separated from at *Rt* 4.9 min in extracts from MoCV1-D-free (C) and MoCV1-D-infected (D) isolates. Within the measured mass spectra, only mass range at 100–300 *m/z* was depicted. Main ions in Fig. 8C at *m/z* 193.0503 $[M–H]^-$ and 175.0390 $[M–H–H2O]^-$ were assigned to chemical fomula C10H9O4 and C10H7O3 by elemental composition analyses on MassLynxTM software, respectively.

shells when they were released into the culture supernatant, thus implying that they were embedded in fragile viral structural proteins or membrane materials. The viral structural proteins might have RNA binding ability, and even if the particle structure collapses, they may still protect the dsRNA molecules for a certain period of time. We do not consider that this outflow phenomenon occurs as a lysis process like a phage, but that MoCV1 is released in the process of cell breakage, with delayed degradation of the dsRNA molecules. Since this is a rare phenomenon in fungal viruses, we would like to examine this process in more depth in future studies.

In the present study, we used HPLC and UPLC-ToF/MS analyses to show that the impaired pigmentation of the MoCV1-D-infected isolate was accompanied by the reduced accumulation of a melanin biosynthesis-related intermediate (Fig. 8). Our data were not quantitative

due to the unavailability of known standard compounds. However, UPLC-ToF-MS is a precise and effective tool for the characterization of unknown compounds. We clearly showed that at least one intermediate related to *M. oryzae* melanin biosynthesis is produced in the MoCV1-D-free isolate but not in the MoCV1-D-infected isolate. Therefore, our results imply that MoCV1-D disturbs melanin biosynthesis in the host cell via a deficiency of scytalone accumulation. Melanization in mycelia and appressoria plays crucial roles in the protection of pathogens from antibiotic stressors and in the pathogenicity of *M. oryzae* to rice (Belozerskaya et al., 2017). In order to further understand the role of melanization in host attenuation by MoCV1-D, we will investigate the accumulation of other intermediates. These trials will contribute to a more general understanding of the mechanisms by which MoCV1-D causes host attenuation, and are currently in progress.

Funding information

This research was supported by a grant from the New Energy and Industrial Technology Development Organization (No. 08C46503c, to H.M.), a grant from the Adaptable and Seamless Technology Transfer Program (No. AS242Z01400N, to H.M.), and by a Grant-in-Aid for Scientific Research (C) from the Japan Society for the Promotion of Science (No. 15K07838, to H.M.). The funders had no role in study design, data collection, or interpretation, or in the decision to submit the work for publication.

Conflict of interest

None.

Acknowledgements

The authors would like to express their gratitude to Mr. Taihei Nagai, Tokyo University of Agriculture and Technology, for his excellent supports of transformation experiment of *Magnaporthe oryzae*.

Appendix A. Supplementary data

Supplementary data to this article can be found online at https://doi.org/10.1016/j.virol.2019.07.014.

References

Ai, Y.P., Zhong, J., Chen, C.Y., Zhu, H.J., Gao, B.D., 2016. A novel single-stranded RNA virus isolated from the rice-pathogenic fungus *Magnaporthe oryzae* with similarity to members of the family *Tombusviridae*. Arch. Virol. 161, 725–729.

Aihara, M., Urayama, S.I., Le, M.T., Katoh, Y., Higashiura, T., Fukuhara, T., Arie, T., Teraoka, T., Komatsu, K., Moriyama, H., 2018. Infection by Magnaporthe oryzae chrysovirus 1 strain A triggers reduced virulence and pathogenic race conversion of it host fungus, *Magnaporthe oryzae*. J. Gen. Plant Pathol. 84, 92–103.

Aoki, N., Moriyama, H., Kodama, M., Arie, T., Teraoka, T., Fukuhara, T., 2009. A novel mycovirus associated with four double-stranded RNAs affects host fungal growth in *Alternaria alternata*. Virus Res. 140, 179–187.

Bao, X., Roossinck, M.J., 2013. Multiplexed interactions: viruses of endophytic fungi. Adv. Virus Res. 86, 37–58.

Belozerskaya, T.A., Gessler, N.N., Aver'yanov, A.A., 2017. In: Merillon, J.,-M., Ramawat, K.G. (Eds.), Melanin Pigments in Fungi. Fungal Metabolites, pp. pp263–291. https://doi.org/10.1007/978-3-319-25001-4_29.

Bormann, J., Heinze, C., Blum, C., Mentges, M., Brockmann, A., Alder, A., Landt, S.K., Josephson, B., Indenbirken, D., Spohn, M., Plitzko, B., Loesgen, S., Freitag, M., Schäfer, W., 2018. Expression of a structural protein of the mycovirus FgV-ch9 negatively affects the transcript level of a novel symptom alleviation factor and causes virus-infection like symptoms in *Fusarium graminearum*. J. Virol. https://doi.org/10.1128/JVI.00326-18.

Darissa, O., Willingmann, P., Schafer, W., Adam, G., 2011. A novel double-stranded RNA mycovirus from *Fusarium graminearum*: nucleic acid sequence and genomic structure. Arch. Virol. 156, 647–658.

Dawe, A.L., Nuss, D.L., 2013. Hypovirus molecular biology: from Koch's postulates to host self-recognition genes that restrict virus transmission. Adv. Virus Res. 86, 109–147.

Du, Y., He, X., Zoug, X., Fang, S., Deng, Q., 2016. Complete nucleotide sequence of *Magnaporthe oryzae* parititivirus. Arch. Virol. 161, 3295–3298.

Ejmal, M.A., Holland, D.J., MacDiarmid, R.M., Pearson, M.N., 2018. The Effect of Aspergillus thermomutatus Chrysovirus 1 on the biology of three *Aspergillus* species. Viruses. https://doi.org/10.3390/v10100539.

Frohman, M.A., Dush, M.K., Martin, G.R., 1988. Rapid production of full-length cDNAs from rare transcripts: amplification using a single gene-specific oligonucleotide primer. Proc. Natl. Acad. Sci. U.S.A. 85, 8998–9002.

Ghabrial, S.A., 2008. Totiviruses. In: third ed. In: Mahy, B.W.J., Van Regenmortel, M.H.V. (Eds.), Encyclopedia of Virology, vol. 1. Elsevier, Oxford, pp. 503–513.

Ghabrial, S.A., Suzuki, N., 2009. Viruses of plant pathogenic fungi. Annu. Rev. Phytopathol. 47, 353–384.

Ghabrial, S.A., Soldevila, A.I., Havens, W.M., 2002. Molecular genetics of the viruses infecting the plant pathogenic fungus Helminthosporium victoriae. In: Tavantzis, S. (Ed.), Molecular Biology of Double-Stranded RNA: Concepts and Applications in Agriculture, Forestry and Medicine, pp. 213–236.

Ghabrial, S.A., Dunn, S.E., Li, H., Xie, J., Baker, T.S., 2013. Viruses of *Helminthosporium* (Cochlioblus) *victoriae*. Adv Virus Res (SanDiego, Elsevier) 86, 289–325.

Ghabrial, S.A., Castón, J.R., Jiang, D., Nibert, M.L., Suzuki, N., 2015. 50-plus years of fungal viruses. Virology 479–480, 356–368.

Ghabrial, S.A., Castón, J.R., Coutts, R.H.A., Hillman, B.I., Jiang, D., Kim, D.H., Moriyama, H., 2018. ICTV virus taxonomy profile: *Chrysoviridae*. J. Gen. Virol. 99, 19–20.

Gietz, R.D., Schiestl, R.H., Willems, A.R., Woods, R.A., 1995. Studies on the transformation of intact yeast cells by the LiAc/SS-DNA/PEG procedure. Yeast 11, 355–360.

Greenblatt, G.A., Wheeler, M.H., 1986. HPLC analysis of fungal melanin intermediates and related metabolites. J. Liq. Chromatogr. 9 (5), 971–981.

Heiniger, U., Rigling, D., 1994. Biological control of chestnut blight in Europe. Annu. Rev. Phytopathol. 32, 581–599.

Hillman, B.I., Cai, G., 2013. The family Narnaviridae: simplest of RNA viruses. Adv. Virus Res. 86, 149–176.

Huang, S., Ghabrial, S.A., 1996. Organization and expression of the double-stranded RNA genome of Helminthosporium victoriae 190S virus, a totivirus infecting a plant pathogenic filamentous fungus. Proc. Natl. Acad. Sci. U.S.A. 93, 12541–12546.

Ikeda, K., Inoue, K., Kida, C., Uwamori, T., Sasaki, A., Kanematsu, S., Park, P., 2013. Potentiation of mycovirus transmission by zinc compounds via attenuation of heterogenic incompatibility in *Rosellinia necatrix*. Appl. Environ. Microbiol. 79, 3684–3691.

Illana, A., Marconi, M., Rodríguez-Romero, J., Xu, P., Dalmay, T., Wilkinson, M.D., Ayllón, M., Sesma, A., 2017. Molecular characterization of a novel ssRNA ourmia-like virus from the rice blast fungus *Magnaporthe oryzae*. Arch. Virol. 162, 891–895.

Jiang, D., Ghabrial, S.A., 2004. Molecular characterization of Penicillium chrysogenum virus: reconsideration of the taxonomy of the genus Chrysovirus. J. Gen. Virol. 85, 2111–2121.

Kamakura, T., Yamaguchi, S., Saitoh, K., Teraoka, T., Yamaguchi, I., 2002. A novel gene, CBP1, encoding a putative extracellular chitin-binding protein, may play an important role in the hydrophobic surface sensing of *Magnaporthe grisea* during appressorium differentiation. Mol. Plant Microbe Interact. 15, 437–444.

Kato, A., Miyake, T., Nishimura, K., Tateishi, H., Teraoka, T., Arie, T., 2012. Use of fluorescent proteins to visualize interactions between the Bakanae disease pathogen *Gibberella fujikuroi* and the biocontrol agent *Talaromyces* sp. KNB-422. J. Gen. Plant Pathol. 78, 54–61.

Komatsu, K., Urayama, S., Katoh, Y., Fuji, S., Hase, S., Fukuhara, T., Arie, T., Teraoka, T., Moriyama, H., 2016. Detection of Magnaporthe oryzae chrysovirus 1 in Japan and establishment of a rapid, sensitive and direct diagnostic method based on reverse transcription loop-mediated isothermal amplification. Arch. Virol. 161, 317–326.

Kumar, S., Stecher, G., Tamura, K., 2016. MEGA7: molecular evolutionary genetics analysis version 7.0 for bigger datasets. Mol. Biol. Evol. 33, 1870–1874.

Kurahashi, Y., Araki, Y., Kinbara, T., Pontzen, R., Yamaguchi, I., 1998. Intermediates accumulation and inhibition sites of carpropamid in the melanin biosynthesis pathway of *Pyricularia oryzae*. J. Pestic. Sci. 23, 22–28.

Le, S.Q., Gascuel, O., 2008. An improved general amino acid replacement matrix. Mol. Biol. Evol. 25, 1307–1320.

Litzenberger, S.C., 1949. Nature of susceptibility to *Helminthosporium victoriae* and resistance to *Puccina coronata* in Victoria oat. Phytopathology 39, 300–318.

Maejima, K., Himeno, M., Komatsu, K., Kakizawa, S., Yamaji, Y., Hamamoto, H., Namba, S., 2008. Complete nucleotide sequence of a new double-stranded RNA virus from the rice blast fungus, *Magnaporthe oryzae*. Arch. Virol. 153, 389–391.

Milgroom, M.G., Cortesi, P., 2004. Biological control of chestnut blight with hypovirulence: a critical analysis. Annu. Rev. Phytopathol. 42, 311–338.

Nibert, M.L., Tang, J., Xie, J., Collier, A.M., Ghabrial, S.A., Baker, T.S., Tao, Y.J., 2013. 3D structures of fungal partitiviruses. Adv. Virus Res. 86, 59–85.

Nicholas, K.B., Nicholas Jr., H.B., Deerfield II., D.W., 1997. GeneDoc: analysis and visualization of genetic variation. Embnet News 4, 1–4.

Nuss, D.L., 2005. Hypovirulence: mycoviruses at the fungal–plant interface. Nat. Rev. Microbiol. 3, 632–642.

Okada, R., Kiyota, E., Moriyama, H., Fukuhara, T., Natsuaki, T., 2015. A simple and rapid method to purify viral dsRNA from plant and fungal tissue. J. Gen. Plant Pathol. 81, 103–107.

Okada, R., Ichinose, S., Takeshita, K., Syun-ichi Urayama, S., Fukuhara, T., Komatsu, K., Arie, T., Ishihara, A., Egusa, M., Kodama, M., Moriyama, H., 2018. Molecular characterization of a novel mycovirus in *Alternaria alternata* manifesting two-sided effects: down-regulation of host growth and up-regulation of host plant pathogenicity. Virology 519, 23–32.

Sanderlin, R.S., Ghabrial, S.A., 1978. Physicochemical properties of two distinct types of virus-like particles from *Helminthosporium victoriae*. Virology 87, 142–151.

Sasaki, A., Nakamura, H., Suzuki, N., Kanematsu, K., 2016. Characterization of a new megabirnavirus that confers hypovirulence with the aid of a co-infecting partitivirus to the host fungus, *Rosellinia necatrix*. Virus Res. 219, 73–82.

Sherman, F., 2002. Getting started with yeast. Methods Enzymol. 350, 3–41.

Tang, L., Hu, Y., Liu, L., Wu, S., Xie, J., Cheng, J., Fu, Y., Zhang, G., Ma, J., Wang, Y., Zhang, L., 2015. Genomic organization of a novel victorivirus from the rice blast fungus *Magnaporthe oryzae*. Arch. Virol. 160, 2907–2910.

Thompson, J.D., Gibson, T.J., Plewniak, F., Jeanmougin, F., Higgins, D.G., 1997. The CLUSTAL X windows interface: flexible strategies for multiple sequence alignment aided by quality analysis tools. Nucleic Acids Res. 25, 4876–4882.

Urayama, S., Kato, S., Suzuki, Y., Aoki, N., Le, M.T., Arie, T., Teraoka, T., Fukuhara, T., Moriyama, H., 2010. Mycoviruses related to chrysovirus affect vegetative growth in the rice blast fungus *Magnaporthe oryzae*. J. Gen. Virol. 91, 3085–3094.

Urayama, S., Ohta, T., Onozuka, N., Sakoda, H., Fukuhara, T., Arie, T., Teraoka, T., Moriyama, H., 2012. Characterization of Magnaporthe oryzae chrysovirus 1 structural proteins and their expression in *Saccharomyces cerevisiae*. J. Virol. 86, 8287–8295.

Urayama, S., Sakoda, H., Takai, R., Katoh, Y., Minh Le, T., Fukuhara, T., Arie, T., Teraoka, T., Moriyama, H., 2014a. A dsRNA mycovirus, Magnaporthe oryzae chrysovirus 1-B, suppresses vegetative growth and development of the rice blast fungus. Virology 448, 265–273.

Urayama, S., Fukuhara, T., Moriyama, H., Toh, E.A., Kawamoto, S., 2014b. Heterologous expression of a gene of Magnaporthe oryzae chrysovirus 1 strain A disrupts growth of the human pathogenic fungus *Cryptococcus neoformans*. Microbiol. Immunol. 58, 294–302.

Urayama, S., Kimura, Y., Katoh, Y., Ohta, T., Onozuka, N., Fukuhara, T., Arie, T., Teraoka, T., Komatsu, K., Moriyama, H., 2016a. Suppressive effects of mycoviral proteins encoded by Magnaporthe oryzae chrysovirus 1 strain A on conidial germination of the rice blast fungus. Virus Res. 223, 10–19.

Urayama, S., Takai, Y.,H., Nonomura, T., 2016b. FLDS: a comprehensive dsRNA sequencing methods for intracellular RNA virus surveillance. Microb. Environ. 31, 33–40.

Watanabe, S., Kumakura, K., Izawa, N., Nagayama, K., Mitachi, T., Kanamori, M., Arie, T., 2007. Mode of action of Trichoderma asperellum SKT-1, a biocontrol agent against *Gibberella fujikuroi*. J. Pestic. Sci. 32, 222–228.

Wheeler, M.H., Greenblatt, G.A., 1988. The inhibition of melanin biosynthetic reactions in *Pyricularia oryzae* by compounds that prevent rice blast disease. Exp. Mycol. 12, 151–160.

Xie, J., Havens, W.M., Lin, Y.H., Suzuki, N., Ghabrial, S.A., 2016. The victorivirus Helminthosporium victoriae virus 190S is the primary cause of disease/hypovirulence in its natural host and a heterologous host. Virus Res. 213, 238–245.

Yang, Y., Zhang, H., Li, G., Li, W., Wang, X. e., Song, F., 2009. Ectopic expression of MgSM1, a Cerato-platanin family protein from *Magnaporthe grisea*, confers broad--spectrum disease resistance in Arabidopsis. Plant Biotechnol. J. 7, 763–777.

Yokoi, T., Yamashita, S., Hibi, T., 2007. The nucleotide sequence and genome organization of Magnaporthe oryzae virus 1. Arch. Virol. 152, 2265–2269.

Yu, X., Li, B., Fu, Y., Xie, J., Cheng, J., Ghabrial, S.A., Li, G., Yi, X., Jiang, D., 2013. Extracellular transmission of a DNA mycovirus and its use as a natural fungicide. Proc. Natl. Acad. Sci. U.S.A. 110, 1452–1457.